

## RELIABILITY-BASED INTERNAL STABILITY DESIGN FOR MSE WALL STRUCTURES

Richard J. Bathurst

Civil Engineering Department, GeoEngineering Centre at Queen's-RMC, Canada. E-mail: [bathurst-r@rmc.ca](mailto:bathurst-r@rmc.ca)

Yoshihisa Miyata

Civil Engineering Department, National Defense Academy, Japan. E-mail: [miyamiya@nda.ac.jp](mailto:miyamiya@nda.ac.jp)

Tony M. Allen

Washington State Department of Transportation, WA, USA. E-mail: [tonyallen1957@gmail.com](mailto:tonyallen1957@gmail.com)

Nezam Bozorgzadeh

Norwegian Geotechnical Institute, Norway. E-mail: [nezam.bozorgzadeh@ngi.no](mailto:nezam.bozorgzadeh@ngi.no)

This paper demonstrates the general approach for reliability-based internal stability design of mechanically stabilized earth (MSE) wall structures using as examples the limit states associated with internal stability of steel strip, steel grid, geogrid and PET strap MSE walls. An important feature of the general approach is a quantitative link to the deterministic factors of safety used in past practice. The calculation of reliability index (or equivalently the probability that the internal limit state is not satisfied) includes the contribution of model method bias and the uncertainty in the estimate of the nominal load and resistance terms in each limit state performance function. The estimate of reliability index can be carried out using Monte Carlo simulation or using a closed-form solution for the case that bias and nominal values are lognormally distributed. The general approach includes the quantitative influence of (model) bias dependencies with nominal values and possible correlations between load and resistance nominal values that are possible when analytical equations for load-side and resistance-side contributions have common input parameters, which themselves have some uncertainty.

*Keywords:* mechanically stabilized earth (MSE) walls, reliability-based design, internal stability.

### 1. Introduction

Much progress has been made to migrate from deterministic internal stability design approaches for mechanically stabilized earth (MSE) wall structures to (probabilistic) reliability-based design. The latter ensures that the margin of safety against not satisfying a particular limit state for a design nominal factor of safety is expressed probabilistically. Deterministic factor-of-safety design, load and resistance factor design (LRFD) and partial factor approaches cannot provide the designer with the actual true probability that a design limit state is satisfied at time of design. A probabilistic approach provides a more nuanced appreciation of margins of safety in this regard. This paper describes the general approach for reliability-based design and analysis for the internal stability limit states for MSE walls constructed with steel strip, steel grid, geogrid and polyester (PET) strap reinforcing layers.

### 2. Preliminaries

Example limit states for polymeric (geosynthetic) and steel reinforced MSE walls are shown in Fig. 1. For MSE walls with extensible polymeric geogrid and polyester (PET) strap reinforcement types, the partition between the active and passive zones is taken as a linear surface computed using Rankine earth pressure theory. For steel strip and steel grid walls the partition is bi-linear. The soil failure limit state applies only to geosynthetic walls when using the stiffness method to compute reinforcement tensile loads (Allen and Bathurst 2015, 2018). The resistance for this limit state is related to the creep-reduced stiffness of the reinforcement (e.g., Bathurst and Allen 2023). From Bathurst and Javankhosdel (2017), the general form of the limit state performance function for each limit state in Fig. 1 can be expressed as:

$$g = \frac{R_m}{Q_m} - 1 = \frac{\lambda_R R_n}{\lambda_Q Q_n} - 1 \quad (1)$$

Here,  $R_m$  and  $Q_m$  are the measured (observed) resistance and measured (observed) load, respectively. Parameters  $\lambda_R$  and  $\lambda_Q$  are resistance and load *method bias* (or *bias* values for brevity), respectively, and are used to transform nominal values ( $R_n$  and  $Q_n$ ) to corresponding measured values, i.e.,  $\lambda_R = R_m/R_n$  and  $\lambda_Q = Q_m/Q_n$ . Nominal load and resistance values have uncertainty and thus these values and corresponding bias values can be treated as random variables in Monte Carlo simulations. Monte Carlo simulation is carried out to compute  $P_f = P(g < 0)$  corresponding to the probability that the limit state is not satisfied (Fig. 2). Alternatively, the corresponding reliability index ( $\beta$ ) can be calculated as  $\beta = -\Phi^{-1}(P_f)$  where  $\Phi^{-1}$  is the inverse of the cumulative distribution function of the standard normal distribution. If all the parameters in Eq. 1 are described

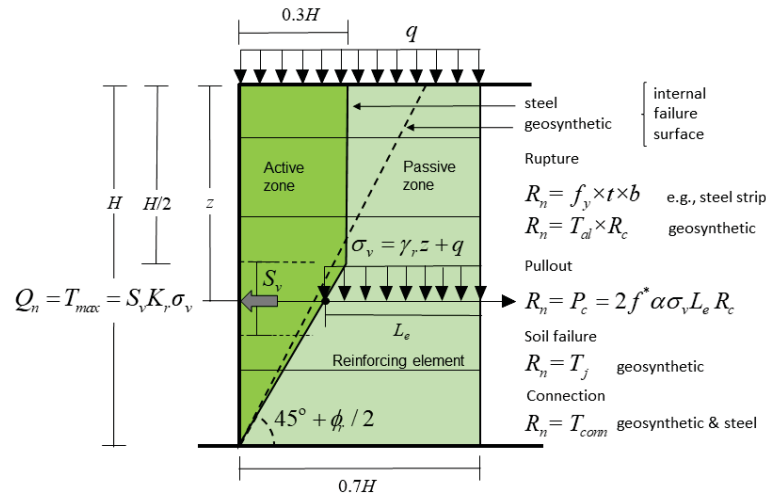


Fig. 1. Internal stability limit states for MSE walls. See Bathurst and Miyata (2024) for definition of symbols.

by lognormal distributions, then  $\beta$  for each limit state can be computed using the following closed-form solution:

$$\beta^2 = A \times \ln(F_n) + B \quad (2)$$

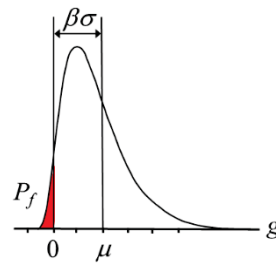


Fig.2. Schematic distribution of limit state (performance)function  $g$ . Note:  $\mu$  and  $\sigma$  are the mean and standard deviation of  $g$ , and  $\beta$  is the reliability index.

where,  $F_n$  is the average nominal factor of safety that is familiar from deterministic allowable stress design (ASD) and is assumed equal to the ratio of the mean estimate of nominal resistance ( $\mu_{R_n}$ ) and mean estimate of nominal load ( $\mu_{Q_n}$ ). The remaining terms are:

$$A = \frac{1}{\sqrt{\ln \left[ \frac{(1 + COV_{Q_n}^2)(1 + COV_{\lambda_Q}^2)(1 + COV_{R_n}^2)(1 + COV_{\lambda_R}^2)(1 + \rho_R COV_{R_n} COV_{\lambda_R})^2 (1 + \rho_Q COV_{Q_n} COV_{\lambda_Q})^2}{(1 + \rho_n COV_{R_n} COV_{Q_n})^2} \right]}} \quad (3)$$

and

$$B = \frac{\ln \left[ \left( \frac{\mu_{\lambda_R}}{\mu_{\lambda_Q}} \right) \sqrt{\frac{(1 + COV_{Q_n}^2)(1 + COV_{\lambda_Q}^2)}{(1 + COV_{R_n}^2)(1 + COV_{\lambda_R}^2)}} \right]}{\sqrt{\ln \left[ \frac{(1 + COV_{Q_n}^2)(1 + COV_{\lambda_Q}^2)(1 + COV_{R_n}^2)(1 + COV_{\lambda_R}^2)(1 + \rho_R COV_{R_n} COV_{\lambda_R})^2 (1 + \rho_Q COV_{Q_n} COV_{\lambda_Q})^2}{(1 + \rho_n COV_{R_n} COV_{Q_n})^2} \right]}} \quad (4)$$

Here, the corresponding coefficients of variation (COV) for the random variables introduced thus far are denoted as  $COV_{R_n}$  for nominal resistance,  $COV_{Q_n}$  for nominal load,  $COV_{\lambda_R}$  for resistance bias, and  $COV_{\lambda_Q}$  for load bias. Parameters  $\rho_R$  and  $\rho_Q$  are Pearson’s correlation coefficients between variables  $R_n$  and  $\lambda_R$ , and between  $Q_n$  and  $\lambda_Q$ , respectively; they are used to quantify bias dependencies with nominal values. Parameter  $\rho_n$  is the correlation coefficient between  $R_n$  and  $Q_n$  and is called nominal correlation;  $\rho_n = 0$  for the tensile strength and soil failure limit states because nominal load values and nominal resistance values are sampled from independent populations. Soil material properties and their statistical characteristics for the pullout limit state are the same for the load equation associated with the active zone in Fig. 1, and the pullout equation associated with the passive zone; hence,  $\rho_n = 0$  and will vary with changes in the distributions for friction angle and unit weight

assumed at the location of each reinforcement layer when one or both parameters appear in load and resistance equations. An important observation from Eq. 2 is that reliability index  $\beta$  varies linearly with nominal factor of safety when all statistical quantities remain the same. Stated alternatively, as the nominal factor of safety is increased at time of design, the margin of safety to satisfy the limit state from a probabilistic point of view increases, which is expected at least intuitively. Because the closed form-solution for  $\beta$  includes the nominal factor of safety, it provides a quantitative link to ASD past practice.

### 3. Selection of bias and nominal values

Load bias values are computed as the measured value from an instrumented layer in a wall divided by the predicted value using a model for the tensile load in a reinforcement layer under operational conditions. There are many different load models that vary with reinforcement type. Pullout bias values are computed by taking the measured pullout capacity from a laboratory pullout box test and dividing it by the predicted value using a pullout model (such as the one shown in Fig. 1) with input parameters that match the pullout test specimen dimensions, vertical stress and soil properties. For the tensile strength limit state, bias is the measured strength from a single test divided by the average of tensile strength from multiple tests carried out on specimens taken from the same sample in accordance with ASTM test protocols. The same is true for the stiffness bias values which are used for the resistance side in the soil failure limit state calculations. The authors have collected large databases of wall reinforcement load measurements from full-scale instrumented MSE walls, laboratory pullout tests, and strength and reinforcement stiffness values from laboratory tensile testing. These data have been used to compile a comprehensive collection of bias statistics for load and resistance models used for internal stability design of MSE walls (e.g., Bathurst and Miyata 2024). The magnitudes of the COV of the nominal values in Eq. 3 and 4 are taken as 0, 0.1, 0.2 and 0.3. The larger the value of  $COV_{R_n}$  and  $COV_{Q_n}$ , the greater the uncertainty in the choice of the nominal value for  $R_n$  and  $Q_n$ , respectively, at the time of design. Bathurst and Javankhoshdel (2017) and Bathurst et al. (2019a,b; 2020) selected the values of 0.1, 0.2 and 0.3 to match notions of high, typical and low project *level of understanding*, respectively, that are adopted in Canadian foundation engineering LRFD practice (CSA 2019; Fenton et al. 2016). A typical level of understanding represents expected typical good project knowledge, experience and design practice. The exception to these values is the use of  $COV_{R_n} = 0$  for the tensile strength and soil failure limit states where the nominal tensile strength and nominal stiffness are taken as deterministic; the uncertainties in the estimate of tensile strength and tensile stiffness are captured by the COV of the resistance bias ( $COV_{\lambda R}$ ) as described above. In US practice, the notion of level of understanding does not appear and hence  $COV_{Q_n} = COV_{R_n} = 0$  (AASHTO 2020).

### 4. Example results

Fig. 3 shows plots of reliability index versus nominal factor of safety which is calculated as the ratio of the best estimate of nominal resistance and best estimate of the nominal load as in ASD past practice explained earlier. The stiffness method (Allen and Bathurst 2015, 2018) load bias statistics were used in these calculations. The plots present as log-linear lines consistent with Eq. 2. For each set of limit state curves the magnitude of  $\beta$  for a given value of  $F_n$  decreases with increasing nominal load uncertainty (i.e., increasing  $COV_{Q_n}$ ). Superimposed on the figure are target reliability index values and the corresponding probabilities that the limit state is not satisfied. Values of  $\beta = 3.09$  and higher can be found in design codes and guidance documents for geotechnical foundation structures. However, the recommended target  $\beta$  for internal ultimate limit states (e.g., tensile, pullout and connection strength) is  $\beta = 2.33$  ( $P(g < 0) = 1/100$ ) (Allen et al. 2005). This relatively small value of  $\beta$  may appear to be too low. However, this value is reasonable given that, internally, MSE walls are highly strength-redundant systems. For example, if one layer does not satisfy an internal stability limit state, neighboring reinforcement layers can compensate. The soil failure limit state applies only to MSE walls with relatively extensible (geosynthetic) reinforcing elements and are designed using the stiffness method. When this limit state is satisfied, the likelihood of a contiguous failure surface developing through the height of the reinforced soil mass is prevented. The stiffness method was calibrated assuming that this is the case. The low target  $\beta = 1.00$  is consistent with a serviceability limit state (see Allen and Bathurst 2015; Bathurst and Allen 2023). To use this figure, the designer first computes the nominal factor of safety for a trial design. The corresponding  $\beta$  value is then computed from Eq. 2 or taken from the figure. If the target  $\beta$  value is not satisfied, then  $F_n$  could be increased by (say) decreasing the reinforcement spacing. If it is the pullout limit state, then  $F_n$  (and thus  $\beta$ ) can be increased by increasing the reinforcement length. The convenience of lognormal distributions for load and resistance terms in the performance function (Eq. 2) is clear. However, for steel strip and steel grid MSE walls the tensile strength of the steel reinforcement is influenced by loss of section due to possible corrosion of the steel after the protective zinc coating is consumed over the design life of the steel. The coupled mechanical-corrosion model that is used for the design of these elements results in complicated truncated strength bias distributions as demonstrated by Allen et al. (2019), Bathurst et al. (2021) and Bozorgzadeh et al. (2020a,b). Therefore, the relationship between  $\beta$  and  $F_n$  can only be determined from Monte Carlo simulation.

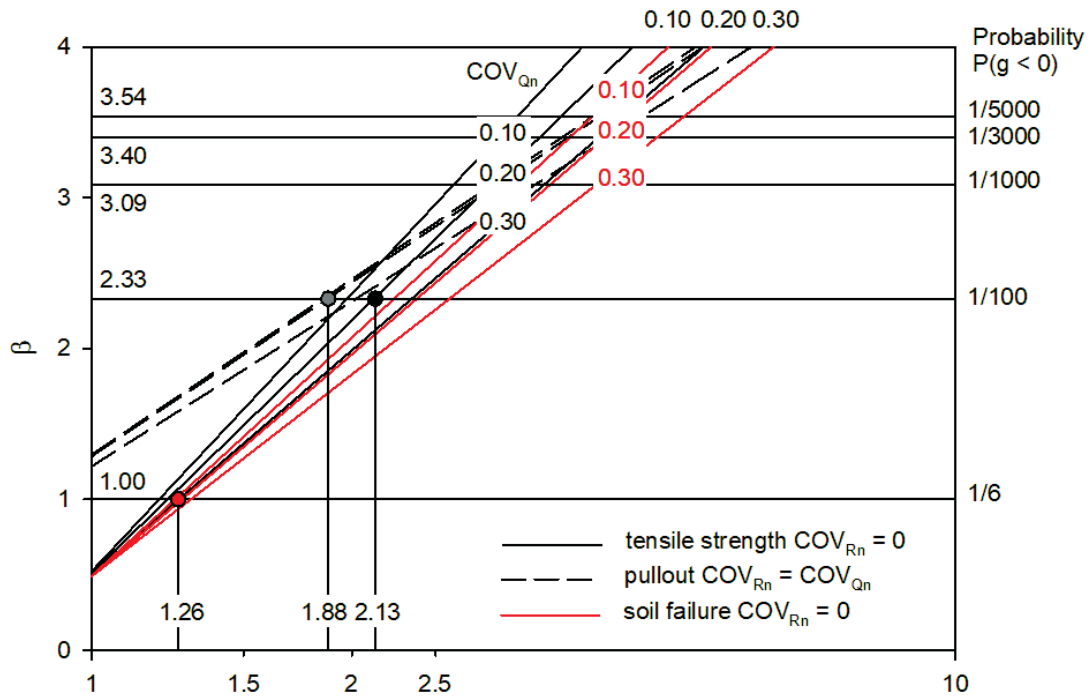


Figure 3. Reliability index ( $\beta$ ) versus nominal factor of safety ( $F_n$ ) for geogrid MSE walls for three internal stability limit states. Load bias statistics correspond to the stiffness method.

## 5. Conclusions

This paper describes the major features of reliability-based internal stability design of MSE walls using load and resistance models found in North American LRFD codes (CSA 2019; AASHTO 2020). The general approach requires that a wall must fall within the envelope of project conditions for the instrumented walls that were used to gather load bias statistics. The same is true for resistance-side bias statistics. When this is the case, the load and resistance bias statistics compiled by the authors can be used to compute  $\beta$  for different limit states. The general approach aligns with the movement towards reliability-based design for geotechnical soil-structure systems.

## References

- Allen, T.M. and R.J. Bathurst (2015). An improved simplified method for prediction of loads in reinforced soil walls. *ASCE Journal of Geotechnical and Geoenvironmental Engineering* 141(11), 04015049.
- Allen, T.M. and R.J. Bathurst (2018). Application of the Simplified Stiffness Method to design of reinforced soil walls. *ASCE Journal of Geotechnical and Geoenvironmental Engineering* 144(5), 04018024.
- Allen, T.M., R.J. Bathurst and N. Bozorgzadeh (2019). Probabilistic tensile strength analysis of steel strips in MSE walls considering corrosion. *ASCE Journal of Geotechnical and Geoenvironmental Engineering* 145(5), 04019016-1-12.
- Allen, T.M., A.S. Nowak and R.J. Bathurst (2005). *Calibration to Determine Load and Resistance Factors for Geotechnical and Structural Design*. Circular E-C079. Transportation Res Board, National Research Council, Washington, D.C., USA.
- AASHTO (2020). *LRFD Bridge Design Specifications, ninth ed.* American Association of State Highway and Transportation Officials (AASHTO).
- Bathurst, R.J. and T.M. Allen (2023). LRFD calibration for soil failure limit state using the Stiffness Method. *Canadian Geotechnical Journal* 60(7), 1006-1014.
- Bathurst, R.J., T.M. Allen, Y. Miyata, S. Javankhoshdel and N. Bozorgzadeh (2019a). Performance-based analysis and design for internal stability of MSE walls. *Georisk* 13(3), 214-225.
- Bathurst, R.J., N. Bozorgzadeh, Y. Miyata, and T.M. Allen (2021). Reliability-based design and analysis for internal limit states of steel grid-reinforced mechanically stabilized earth walls. *Canadian Geotechnical Journal* 58 (5), 695-710.
- Bathurst, R.J. and S. Javankhoshdel (2017). Influence of model type, bias and input parameter variability on reliability analysis for simple limit states in soil-structure interaction problems. *Georisk* 11(1), 42-54.
- Bathurst, R.J., P. Lin. and T.M. Allen (2019b). Reliability-based design of internal limit states for mechanically stabilized earth walls using geosynthetic reinforcement. *Canadian Geotechnical Journal* 56(6), 774-788.
- Bathurst, R.J. and Y. Miyata (2024). Mechanically stabilized earth (MSE) walls. Chapter 14. In *Data-centric Geotechnics. Geotechnical Structures* (2). K.K. Phoon and C. Tang (Eds). Taylor & Francis Group, LLC, 17 p.
- Bathurst, R.J. Y. Miyata and T.M. Allen (2020). Deterministic and probabilistic assessment of margins of safety for internal stability of as-built PET strap reinforced soil walls. *Geotextiles and Geomembranes* 48(6), 780-792.

- Bozorgzadeh, N., R.J. Bathurst and T.M. Allen. (2020a). Influence of corrosion on reliability-based design of steel grid MSE walls. *Structural Safety* 84: 101914.
- Bozorgzadeh, N., R.J. Bathurst, T.M. Allen and Y. Miyata (2020b). Reliability-based analysis of internal limit states for MSE walls using steel strip reinforcement. *ASCE J of Geotechnical and Geoenvironmental Engineering* 146(1), 0401911.
- CSA (2019). *Canadian Highway Bridge Design Code. CAN/CSA-S6-19*. Canadian Standards Association (CSA).
- Fenton, G.A., F. Naghibi, D. Dundas, R.J. Bathurst and D.V. Griffiths (2016). Reliability-based geotechnical design in the 2014 Canadian Highway Bridge Design Code. *Canadian Geotechnical Journal* 53(2), 236-251.